



Contents lists available at ScienceDirect

Methods

journal homepage: www.elsevier.com/locate/ymeth

Simultaneous flow cytometric immunophenotyping of necroptosis, apoptosis and RIP1-dependent apoptosis

H.L. Lee^a, R. Pike^b, M.H.A. Chong^a, A. Vossenkamper^a, G. Warnes^{c,*}

^a Centre for Immunobiology, Blizard Institute

^b Flow Cytometry Core Facility, John Vane Science Centre

^c Flow Cytometry Core Facility, Blizard Institute, Barts & The London Schools of Medicine & Dentistry, Queen Mary University of London, 4 Newark Street, London E1 2AT, UK

ARTICLE INFO

Article history:

Received 26 June 2017

Received in revised form 22 September 2017

Accepted 30 October 2017

Available online xxx

Keywords:

Flow cytometry

Necroptosis

RIP3, RIP1-Dependent Apoptosis

Apoptosis

ABSTRACT

Flow cytometry was been widely used to measure apoptosis for many decades but the researcher has no definitive way of determining other forms of cell death using this technology. The use of Western Blot technology has numerous drawbacks in that all the cells in the sample whether live, dead or maybe undergoing multiple discrete forms of cell death are analysed as one population. Flow cytometry given that it can analyse different sub-populations of cells within a sample would reveal the expression of cell death markers within these sub-populations rather than just give a single result from the entire population. Here we describe a flow cytometric assay fully realising that potential by the use of anti-RIP-3 (Receptor-interacting serine/threonine-protein kinase 3) and anti-active caspase-3 fluorescently tagged antibodies and a fixable live dead fluorescent dye. This allows the determination of the degree of necroptosis, apoptosis and RIP1-dependent apoptosis within live and dead populations. Necroptosis was identified by the up-regulation of RIP3, while RIP1-dependent apoptosis was described by double positive for RIP3/active Caspase-3 events in live and dead populations. Apoptotic cells were defined by an active-Caspase-3^{ve}/RIP3^{ve} phenotype. Pan-caspase blocker zVAD and RIP1 inhibitors GSK481 or necrostatin-1 revealed interesting modulations of such sub-populations of Jurkat cells. This novel flow cytometric assay employing two antibodies and a fixable viability probe provides the researcher with in-depth analysis of various forms of regulated forms of cell death beyond what is currently available and is a major methodological advancement in this field.

© 2017 Elsevier Inc. All rights reserved.

1. Introduction

The old format of using numbers to classify cell death, Type I being programmed cell death or apoptosis and necroptosis, Type II being autophagy and Type III being necrosis or oncosis had been used for some considerable time and thus the recent reclassification by the NCCD is welcomed [1–4]. The new classification highlights the ‘state of the art’ and the complexity of cell death processes [5]. The new format uses the terminology of Programmed Cell Death (PCD) to only include developmental and homeostatic apoptosis. While oncosis, the correct name for the process of necrosis (dead cells could have arrived in this state from any of the cell death processes), has been properly included as Accidental Cell Death (ACD). All other forms of cell death include classic caspase dependent apoptosis, RIP1 dependent apoptosis, necroptosis, pyroptosis, ferroptosis, parthanatos and autophagy

and have been termed Regulated Cell Death (RCD) [5]. Regulated forms of cell death such as apoptosis and necroptosis are morphologically distinct in that the cell during apoptosis forms blebs on their surface and undergoes DNA fragmentation [1–3,6]. While necroptosis involves the swelling of the cell and organelles with consequent rupture of the cell without significant change to the DNA [7].

Biochemically there are numerous pathways involved in both of these forms of cell death, with apoptosis having an intrinsic route initiated by numerous activating agents such as UV-irradiation, TNF α , etoposide and staurosporine. This also involves the depolarization of the mitochondrial inner membrane resulting in dysfunctionality and release of cytochrome *c* to the cytosol where it binds to Apaf-1 recruiting pro-caspase-9 in an ATP dependent manner to form the apoptosome. This complex activates Caspase-9 which in turn activates effector caspases, which result in fragmentation of the DNA, cell shrinkage, membrane blebbing and the formation of apoptotic bodies [8].

* Corresponding author.

E-mail address: g.warnes@qmul.ac.uk (G. Warnes).

The other route apoptosis can take is the extrinsic route by which TNF α binds to TNFR1 and TNFR2 with signalling via the TRADD death receptor or Fas ligand (Fas L) binding to the Fas receptor. This results in the formation of DISC (Death Inducing Signalling Complex) which contains FADD and caspases 8 and 10 [6,9]. This complex activates caspase-3 which again leads to cell death via apoptosis (complex IIa) [10]. This activation route can also involve RIP1 (Receptor-interacting serine/threonine-protein kinase 1), RIP3 and caspases resulting in RIP1-dependent apoptosis via complex IIb [6,10–12]. Cell death via this cell death receptor route can also bypass the requirement for caspase activation resulting in RIP1 activation and up-regulation of RIP3 resulting in the formation of the so-called ‘necrosome’ or complex IIc with the generation of ROS by mitochondria resulting in cell death via necroptosis [5,6,10,11].

The occurrence and mechanisms of RCD has been in the main confirmed by the use of Western Blot technology. This approach has investigated a particular form of RCD with the use of various activators and inhibitors to determine the signalling pathways involved and the interconnection of numerous forms of RCD e.g. apoptosis, necroptosis and autophagy [13,14].

Unfortunately only Western Blot and microscopy technology can be used to investigate cell death in an adequate manner. In the main flow cytometry as a technology has been left behind in that currently only apoptosis and associated processes can be measured. These processes include plasma membrane integrity, phosphatidylserine (PS) flipping, mitochondrial dysfunction, Reactive Oxygen Species (ROS) generation, DNA fragmentation and damage [13,15–19]. However, none of these flow cytometric techniques actually detects nor measures the numerous specific forms of cell death. Given the knowledge of the proteins involved in signalling pathways and some of their interconnections between the various forms of RCD and the availability of antibodies to such proteins (usually for Western Blotting only) these could be used to semi-quantitate the numerous forms of RCD by flow cytometry. This would perhaps bring flow cytometry to the fore again in studying the interconnections of the numerous forms of RCD in that it may show the presence of immunophenotypically functionally different sub-populations within live and dead cell populations and would shed new light on the mechanisms and the interactivity involved in apoptosis and necroptosis.

Here we describe such an approach by the use of intracellular labelling of RCD signalling proteins, allowing the degree of apoptosis, RIP1-dependent apoptosis and necroptosis in viable and dead cells to be measured flow cytometrically. The processes of apoptosis and necroptosis are known to take several hours to more than 24 h depending on the inducer employed and so the 24 h time point was employed in this study [20–23]. The assay employs a fixable cell viability dye and anti-active caspase-3 and anti-RIP3 which allows the identification of live cells undergoing apoptosis (Caspase-3⁺/RIP3⁻) and necroptosis (up-regulated RIP3 on RIP3⁺/Caspase-3⁻ events) as well as RIP1 dependent apoptosis (RIP3⁺/Caspase-3⁺). RIP3 is always present with RIP1 so it is assumed that such double positive cells are undergoing RIP1-dependent cell death [10]. Equally it is possible to determine the signalling route by which necrotic cells died. So fixable viability dye⁺/Caspase-3⁺ cells have died via apoptosis; only RIP3⁺ cells have died via necroptosis. Double positive cells for Caspase-3 and RIP3 have died via RIP1-dependent apoptosis.

Here we show that TNF α and the necroptotic drug shikonin can induce multiple forms of cell death in a single culture of a cell line. The use of pan-caspase inhibitor, zVAD and RIP1 inhibitors, GSK481 or necrostatin-1 followed by treatment with TNF α or necroptotic drug shikonin appeared to show clearly functional phenotypic distributions within sub-populations. Here we show the pathways that are activated in a single population of cells

can be induced to undergo necroptosis but also showed high levels of classic and RIP1-dependent apoptosis. This new flow cytometric approach to the study of multiple forms of RCD simultaneously employing low numbers of cells compared to that used in Western Blots opens the possibility of screening leucocytes and other cell types from patient tissues *ex vivo*.

2. Materials and methods

2.1. Induction of necroptosis, RIP1-dependent apoptosis and apoptosis

Jurkat cells (human acute T cell leukaemia cell line) were used as a model to study necroptosis, RIP1-dependent apoptosis and apoptosis. Cells were left untreated or treated with TNF α (100 ng/ml, PeproTech, UK), shikonin for 24 h (0.5 μ M, Santa Cruz, USA). Cells were also pre-treated with necroptosis blockers RIP1 inhibitor GSK481 (GSK, UK, 300 nM) or necrostatin-1 (60 μ M Cambridge Bioscience, UK) for 2 h before TNF α or shikonin treatment. Such cells with blocked necroptosis are thus directed to apoptosis which should be enhanced compared to drug treatment alone, see Table 1. Pre-treatment for 2 h with pan-caspase blocker zVAD (20 μ M, Enzo Life Sciences, USA) before TNF α or shikonin treatment should block apoptosis and thus direct the cells to necroptosis, see Table 1. Etoposide (1 μ M, Cambridge Bioscience, UK) was employed to induce apoptosis after 24 h, which was then also blocked by pre-treatment with zVAD for 2 h, see Table 1.

2.2. Annexin V assay

After 24 h cells were harvested and pelleted. Viable cell counts were determined using propidium iodide (5 μ g/ml) with fluorescence collected on a 615/24 nm detector from the 488 nm laser (ACEA Biosciences Novocyte 3000 flow cytometer fitted with a NovoSampler, San Diego, USA) and an absolute cell count measured in a 100 μ l volume. Cells were adjusted to 0.5×10^6 /ml and incubated for 15 min at 37 $^{\circ}$ C with 2.5 μ M DRAQ7 (Biostatus, UK). Washed cells were placed in 400 μ l Annexin V buffer (BD Biosciences, UK) and 2 μ l annexin V-PE (BioLegend, UK) for 15 min at RT. Cells were analysed on a ACEA Biosciences Novocyte 3000 flow cytometer using the 585/40 nm detector for Annexin V-PE. DRAQ7 was excited by the 633 nm laser using the 780/60 nm detector, 20,000 events were collected. Single colour controls were employed to determine the colour compensation using the pre-set voltages on the instrument using Novo Express software (ver 1.2, ACEA Biosciences, USA). Cells were gated on FSC vs SSC removing the small debris near the origin. This was followed by gating on a dot-plot of annexin V-PE vs DRAQ7 with a quadrant placed marking off live cells in the double negative quadrant (lower left), with Annexin V positive or ⁺/DRAQ7 negative or ⁻ (lower right) indicating apoptotic cells and lastly with Annexin V⁺/DRAQ7⁺ and Annexin V⁻/DRAQ7⁺ upper quadrants indicating dead cells (see Supplementary Fig. 1).

2.3. RIP3-Caspase-3 assay

Harvested cells were labelled with fixable live dead stain, Zombie NIR (Near Infra-Red) (BioLegend, UK) at RT for 15 mins. Cells were then washed in PBS/BSA and pellets fixed in Solution A (CalTag, UK) for 15 min at RT. Washed cells were permeabilised in 0.25% Triton X-100 (Sigma, UK) for 15 min at RT. Washed cells (0.5×10^6) were then labelled anti-RIP3-PE (2 μ l, clone B-2, Cat. No. sc-374639, Santa Cruz, USA), and anti-active caspase-3-BV650 (2 μ l, clone C92-605, Cat. No. 564096, BD Biosciences, USA) for 20 min at RT. Washed cells were resuspended in 400 μ l PBS and analysed on a ACEA Bioscience Novocyte 3000 flow

Table 1
Expected forms of cell death.

Inducer	Induced Cell Death Process	+GSK'481	+Necrostatin-1	+zVAD
TNF α	Apoptosis-Necroptosis	Apoptosis	Apoptosis	Necroptosis
Shikonin	Necroptosis-Apoptosis	Apoptosis	Apoptosis	Necroptosis
Etoposide	Apoptosis	ND	ND	None

The cell death inducers, TNF α and shikonin are known to induce both apoptosis and necroptosis to varying degrees in different cell types. Etoposide induces apoptosis, while blockade of necroptosis by pre-treatment with GSK'481 or necrostatin-1 causes increased levels of detectable apoptosis induced by TNF α and shikonin. Pre-treatment with zVAD before TNF α and shikonin causes increased levels of necroptosis. While pre-treatment with zVAD before etoposide causes less cell death. ND – Not Done.

cytometer (30,000 events). Zombie NIR was excited by the 633 nm laser and collected in the 780/60 nm detector. Caspase-3-BV650 was excited by the 405 nm laser and collected at 675/30 nm. RIP3-PE was excited by the 488 nm laser and collected at 585/40 nm. Single colour controls were employed to determine the colour compensation using the pre-set voltages on the instrument using Novo Express software (ver 1.2, ACEA Biosciences, USA). Cells were gated on FSC vs SSC removing the small debris near the origin. Cells were then gated on a dot-plot of Caspase-3-BV650 vs Zombie NIR with a quadrant placed marking off live cells in the double negative quadrant (lower left), with Caspase-3-BV650⁺/Zombie NIR^{-ve} (lower right) indicating apoptotic cells and lastly with Caspase-3-BV650⁺/Zombie NIR⁺ and Caspase-3-BV650^{-ve}/Zombie NIR⁺ upper quadrants indicating dead cells (see Fig. 1). Live and dead cells were gated separately and analysed in RIP3 vs Caspase-3 dot-plots with RIP3⁺/Caspase-3^{-ve} indicating normal resting cells or necroptosis when RIP3 was up-regulated, see Table 2 for a full description of live and dead cell phenotypes. While RIP3^{-ve}/Caspase-3⁺ cells indicate those that have undergone apoptosis. Double negative cells were assumed to have died via a non-apoptotic-necroptotic route. Double positive events indicate cells of the RIP1-dependent apoptosis phenotype in live and dead cells, see Table 2. This is an assumed observation, as RIP3 is associated with RIP1 in the formation of the necrosome [10] (RIP1 and RIP3 was observed to be present in PBMNC, data not shown).

2.4. Imagestream analysis of RIP3-Caspase-3 assay

Cells (2×10^6) were labelled as above except that anti-active caspase-3-BV605 (clone C92-605, BD Biosciences, USA) was employed instead of the BV650 antibody. Single colour controls were employed to set the compensation on the Imagestream MKII instrument (Merck Millipore, UK) using Side Scatter gain set to 2.0, using 488 nm (150 mW), 642 nm (150 mW) and 405 nm lasers (120 mW) using 577/25, 762/35 nm and 610/30 nm filters respectively. 10,000 events were collected (using INSPIRE Software, Merck Millipore, UK) employing the 40x objective, lowest speed and fluorescence gating employed as in flow cytometry using IDEAS software (ver 6.0, Merck Millipore, UK). Single cells were gated using an Area (M01) vs Aspect Ratio (M01) dot-plot (Supplementary Fig. 2A). Focussed cells were gated using the Gradient RMS M01 Channel (Supplementary Fig. 2B). Other gating was carried out as in standard flow cytometry using Caspase-3-BV605 vs Zombie NIR dot-plots (Supplementary Fig. 2C). Further gating on live and dead cells using a Caspase-3-BV605 and RIP3-PE dot-plot was used to gate upon RIP3⁺/Caspase-3^{-ve} (resting cells or necroptosis), double negative (non-apoptotic-necroptotic phenotype), double positive (RIP1 dependent apoptosis) and RIP3^{-ve}/Caspase-3⁺ (apoptotic cells) as described (Supplementary Fig. 2D, E, Table 2).

Imagestream analysis was used to image RIP3 for median fluorescence Intensity and Bright Detail Intensity (BDI, spot fluorescence intensity), Caspase-3, Zombie NIR and cell morphology and RIP3 fluorescence Texture parameters, which included perimeter, cell diameter, circularity, contrast (pixel variation within a cell),

energy (measures intensity concentration), entropy (measures randomness of spots), variance (measures variation of spread of pixel values) and homogeneity (spread of pixel intensities) respectively. Only RIP3 fluorescence median intensity was found to be significantly different within populations so this was the only parameter used to analyse RIP3-PE fluorescence. Of the morphological characteristics these were all lower only in the apoptotic (RIP3^{-ve}/Caspase-3⁺) population as previously reported but this was found to be the case after all treatments employed in this study [24]. Thus morphological analysis did not offer anything unique for analysing the other forms of cell death under investigation so these parameters were not used in this study.

2.5. Statistics

Student *t* tests were performed in GraphPad software Inc., USA with $P = >.05$ not considered significant (NS), $P = <.05^*$, $P = <.01^{**}$.

3. Results

3.1. Annexin V and caspase-3 analysis of apoptosis and necroptosis, and RIP1-dependent apoptosis

The use of the caspase-3 mAb on fixed samples showed the limitation of the annexin V assay, in that anti-active caspase-3 appears to be more sensitive than annexin V and generally detects more apoptotic cells (see Supplementary Fig. 1, Fig. 1). This antibody also specifically indicates the mode of cell death either by apoptosis or necroptosis by being \pm caspase-3 plus viability marker respectively were annexin V does not specifically indicate the form of cell death (see Supplementary Fig. 1, Fig. 1). The Caspase-3-Zombie assay showed that TNF α ±RIP1 inhibitor GSK'481 [25] induced apoptosis to a higher level than seen in Annexin V assay ($25.8 \pm 5\%$, $18 \pm 2.2\%$, Caspase-3⁺/Zombie^{-ve}) as well as necroptosis respectively ($9.5 \pm 1.8\%$, $6.5 \pm 2.96\%$, Caspase-3^{-ve}/Zombie⁺, Supplementary Fig. 1A–C, Fig. 1A–C, Table 2). Inhibition of TNF α induced necroptosis by necrostatin-1 was marginally more efficient than with RIP1 inhibitor GSK'481 with a higher level of apoptosis detected by annexin V and caspase-3 staining ($11.3 \pm 2.6\%$, $19.3 \pm 5.1\%$, Supplementary Fig. 1D, Fig. 1D, Table 1). Pre-treatment of Jurkat cells with pan caspase blocker zVAD before TNF α treatment showed that apoptosis and cell death was blocked to control levels in both assays (Supplementary Fig. 1A, E, Fig. 1A, E, Table 1).

Shikonin, a known inducer of necroptosis was shown to increase the levels of apoptosis (Caspase-3⁺/Zombie^{-ve}, $33.8 \pm 9.9\%$, Fig. 1F) with cell death by necroptosis (Caspase-3^{-ve}/Zombie⁺) being shown to be relatively high at $9 \pm 3.8\%$ (Fig. 1F, Table 1). In contrast such cells labelled with annexin V showed a low level of apoptosis and consequent high level of live cells (Supplementary Fig. 1F). Shikonin plus RIP1 inhibitor GSK'481 (unlike with TNF α plus GSK'481) showed as expected a large increase in apoptosis with Annexin V⁺/DRAQ7^{-ve} or Caspase-3⁺/Zombie^{-ve} ($28.7 \pm 9.4\%$, $44 \pm 5.9\%$); there was also no major change in the dead cell population labelled with Annexin V⁺/DRAQ7⁺ or Caspase-3⁺/Zombie⁺ respectively ($26.3 \pm 3.5\%$, $16.7 \pm 2.1\%$, Supplementary

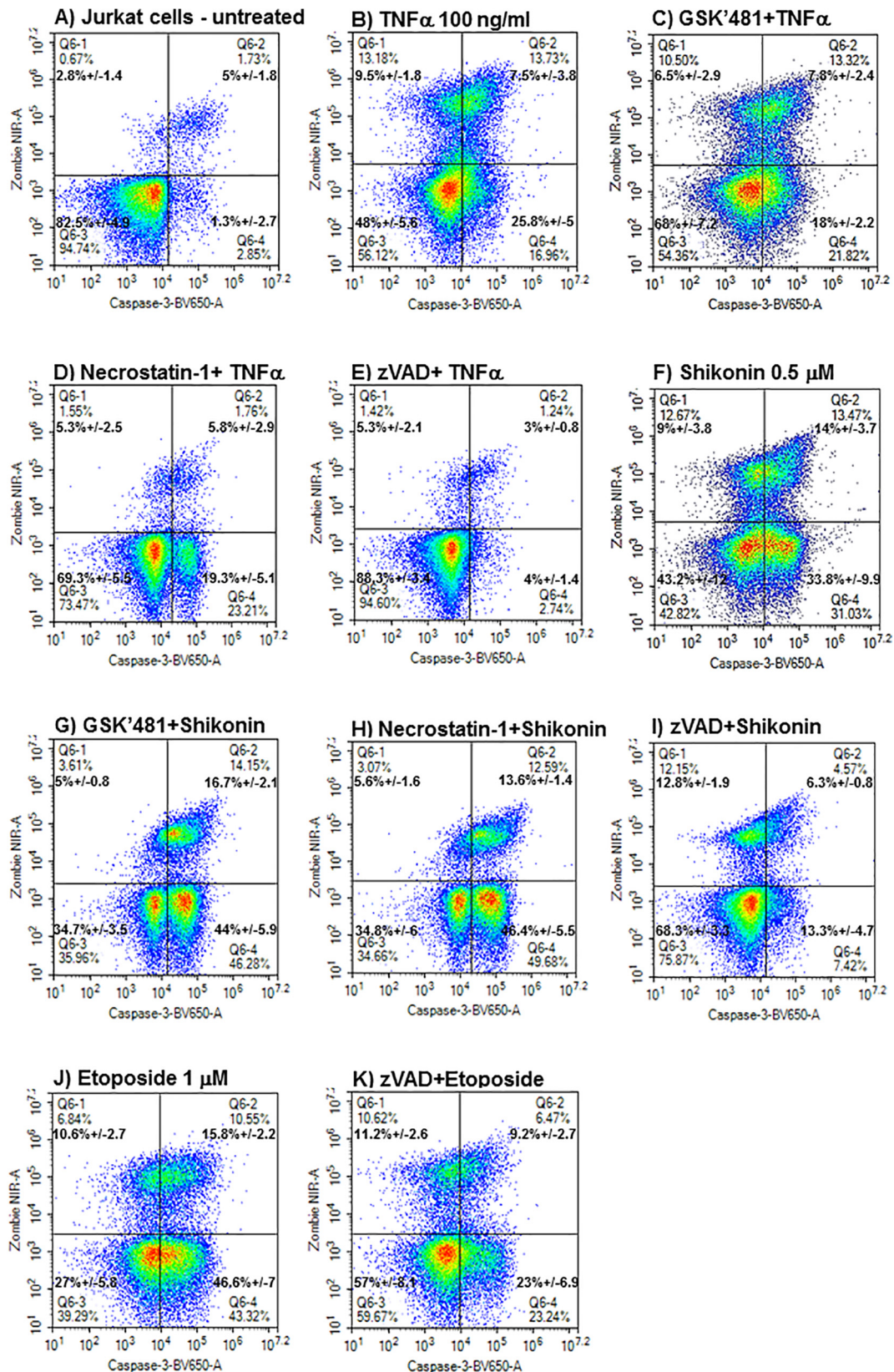


Fig. 1. Cells from all treatments were labelled with Caspase-3-BV650 and cell viability marker, Zombie NIR as described in Materials and Methods. Cells were first gated on FSC-A vs SSC-A to include all data points except cell debris. These cells were then gated employing Caspase-3-BV650 vs Zombie NIR dot-plots to show the percentage live cells (Caspase-3-BV650^{-ve}/Zombie NIR^{-ve}), apoptotic cells (Caspase-3-BV650^{ve}/Zombie NIR^{-ve}), and dead cell populations (Caspase-3-BV650^{ve}/Zombie NIR^{ve} and Caspase-3-BV650^{ve}/Zombie NIR^{ve}). Cell sample preparations analysed were untreated (A), TNF α (100 ng/ml) (B), RIP1 inhibitor GSK'481 (300 nM) plus TNF α (100 ng/ml) (C), necrostatin-1 (60 μ M) plus TNF α (100 ng/ml) (D), zVAD (20 μ M) plus TNF α (100 ng/ml) (E), shikonin (0.5 μ M) (F), RIP1 inhibitor GSK'481 (300 nM) plus shikonin (0.5 μ M) (G), necrostatin-1 (60 μ M) plus shikonin (0.5 μ M) (H), zVAD (20 μ M) plus shikonin (0.5 μ M) (I), etoposide (1 μ M) (J), zVAD (20 μ M) plus etoposide (1 μ M) (K). Mean percentage values were expressed as % \pm SEM for n = 3.

Table 2
Phenotype definitions.

Phenotype	Live cells	Dead cells
RIP3 ⁺ high/Caspase-3 ^{-ve}	Necroptosis	Necroptosis
Caspase-3 ⁺ ve/RIP3 ^{-ve}	Classic Apoptosis	Classic Apoptosis
RIP3 ⁺ ve/Caspase-3 ⁺ ve	RIP1-dependent Apoptosis	RIP1-dependent Apoptosis
RIP3 ^{-ve} /Caspase-3 ^{-ve}	Non apoptotic-necroptotic	Non apoptotic-necroptotic

The phenotypes of cells indicate the form of cell death the cell population were undergoing in live and dead cells. RIP3⁺high/Caspase-3^{-ve} indicated the presence of necroptosis; Caspase-3⁺ve/RIP3^{-ve} indicated the presence of classic apoptosis; RIP3⁺ve/Caspase-3⁺ve indicated the presence of RIP1-dependent apoptosis. While RIP3^{-ve}/Caspase-3^{-ve} indicated cells that have undergone a form of cell death that was non apoptotic-necroptotic.

Fig. 1G, Fig. 1G, Table 1). Necrostatin-1 plus shikonin also showed a similar rise in apoptosis with the Annexin V⁺ve/DRAQ7^{-ve} or Caspase-3⁺ve/Zombie^{-ve} (32.3 ± 1.6%, 46.4 ± 5.5), as well as dead cells (Annexin V⁺ve/DRAQ7⁺ve, 38.8 ± 6.9%) compared to that induced by the RIP1 inhibitor, GSK'481 (Supplementary Fig. 1H, Fig. 1H, Table 1).

As expected pre-treatment of shikonin cultures with zVAD reduced the incidence of apoptotic cells by Caspase-3⁺ve/Zombie^{-ve} (13.3 ± 4.7%) and in the Annexin V assay (9.3 ± 2.3%. Fig. 1I, Supplementary Fig. 1I, Table 1). A large increase in dead cells was also observed (Annexin V⁺ve/DRAQ7⁺ve) above that with shikonin treatment alone (39.3 ± 4.6%, Supplementary Fig. 2I). The dead cells labelled in the Caspase-3/Zombie assay showed as expected a high degree of necroptotic cell death (Caspase-3^{-ve}/Zombie⁺ve, 12.8 ± 1.9%, Fig. 1I).

Etoposide induced apoptosis with a large increase in Annexin V⁺ve/DRAQ7^{-ve} or Caspase-3⁺ve/Zombie^{-ve} (25.8 ± 4.3%, 46.6 ± 7%) and cell death (43.4 ± 3.8%, 15.8 ± 2.2%, Supplementary Fig. 1J, Fig. 1J, Table 1). The action of etoposide was blocked by pre-treatment with zVAD with the apoptotic population falling to 15.6 ± 1.9% with annexin V and 23 ± 6.9% with Caspase-3 (Supplementary Fig. 1K, Fig. 1K, Table 1).

3.2. Flow cytometric and Imagestream RIP3-Caspase-3 analysis of apoptosis, necroptosis, and RIP1-dependent apoptosis

The fixable cell viability dye and anti-caspase-3 antibody was used together with the intracellular detection of RIP3 to identify cells undergoing necroptosis, RIP1-dependent apoptosis as well as apoptosis, see Fig. 2. After gating as described in Materials & Methods 2.2 untreated Jurkat cells showed the distribution of the phenotypes of live and dead cells, resting cells (or necroptosis phenotype when up-regulated RIP3 as indicated by the low level MFI 185,996 ± 6245 in RIP3⁺ve/Caspase-3^{-ve}, 77% ± 4, 9.3% ± 3.3), apoptosis (RIP3^{-ve}/Caspase-3⁺ve, 3.5% ± 1.6, 33.8 ± 9.4%), RIP1-dependent apoptosis (RIP3⁺ve/Caspase-3⁺ve, 7.8% ± 1.7, 36.3% ± 5%) and a double negative phenotype respectively (12.5% ± 6.6, 21% ± 5.2, see Fig. 2A, B, Table 2).

Treatment with TNF α lead to an increase in the RIP3^{-ve}/Caspase-3⁺ve phenotype compared to the control live cells (16.8 ± 3.5% Fig. 2C, Tables 1, 2). Although there was no change in the incidence of the RIP3⁺ve population the level of RIP3 expression (MFI 249,281 ± 31,542) as detected by flow and image cytometry (MFI 233,000 ± 34,200) was increased by 34 ± 10% and 55 ± 15% respectively indicating that these cells had undergone necroptosis, see Figs. 2C, 3.

Imagestream analysis of live TNF α treated cells undergoing RIP1-dependent apoptosis (RIP3⁺ve/Caspase-3⁺ve) or apoptosis (RIP3^{-ve}/Caspase-3⁺ve) showed the presence of RIP3, caspase-3 and a more

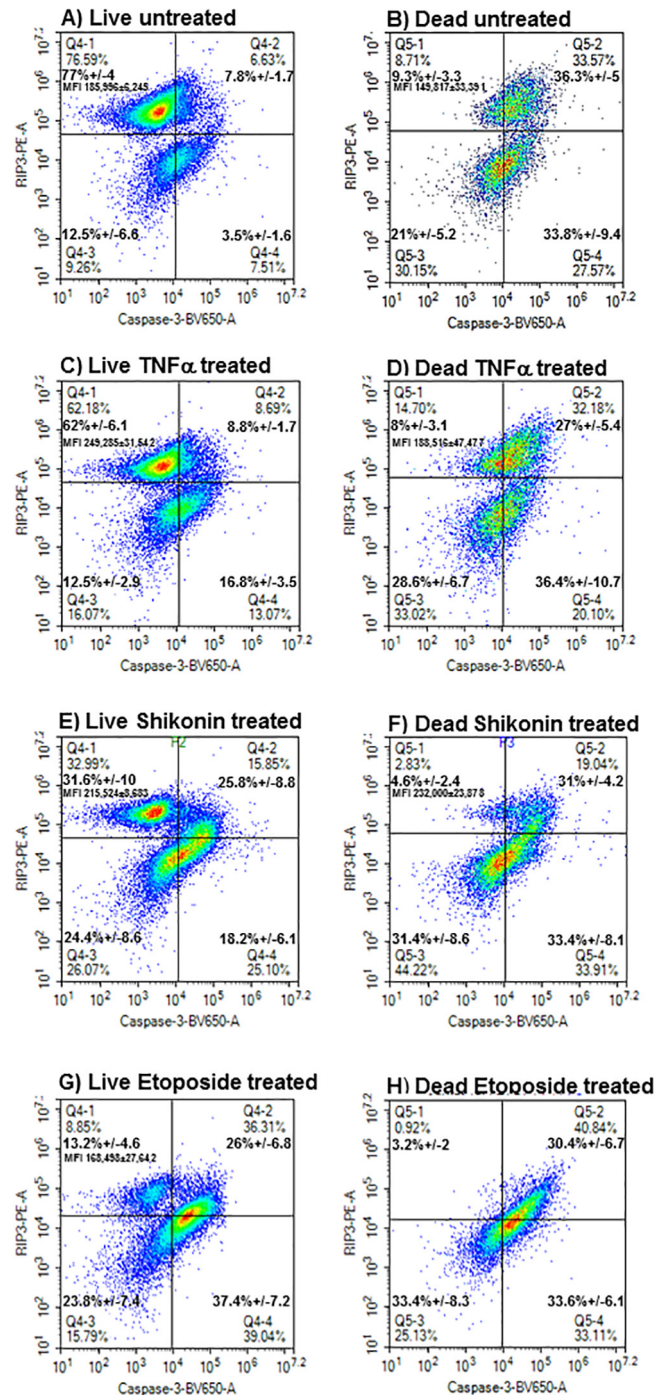


Fig. 2. Untreated cells (A), (B), or TNF α (100 ng/ml) (C), (D) or shikonin (0.5 μ M) (E), (F) or etoposide (1 μ M) (G), (H) were used to induce necroptosis and apoptosis and were labelled with fixable live cell stain Zombie NIR, Caspase-3-BV650 and RIP3-PE as described in Materials and Methods. After gating as described in Fig. 1, live and dead cells were further gated for necroptosis, RIP1-dependent apoptosis and apoptosis respectively using a dot-plot of RIP3-PE vs Caspase-3-BV650 parameters. Necroptosis was described as an up-regulation of RIP3 in the RIP3-PE⁺ve/Caspase-3-BV650^{-ve} population (MFI ± SEM, n = 3). RIP1-dependent apoptosis and apoptosis was described as the RIP3-PE⁺ve/Caspase-3-BV650⁺ve or RIP3-PE^{-ve}/Caspase-3-BV650⁺ve population respectively. Mean percentage values were expressed as % ± SEM for n = 3.

granular or blebbing morphology changes associated with necroptosis or apoptosis respectively (Fig. 4A, C, Supplementary Fig. 4A, C). Further image analysis of all populations of cells showed reductions in cell diameter, perimeter and circularity in the apoptotic (RIP3^{-ve}/Caspase-3⁺ve) population only (data not shown).

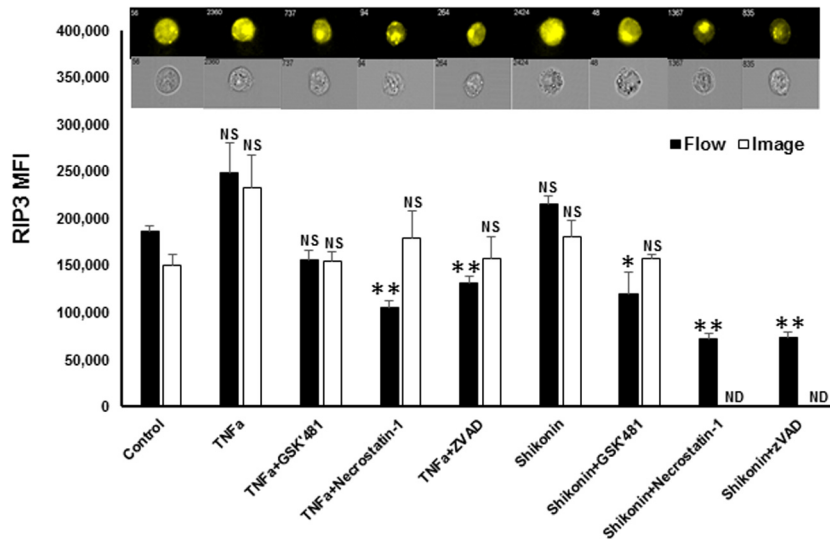


Fig. 3. Cells were untreated, or treated with TNF α (100 ng/ml), or pre-treated with RIP1 inhibitor GSK481 (300 nM) for 2 h followed by TNF α (100 ng/ml), or necrostatin-1 for 2 h followed by TNF α (100 ng/ml), or zVAD for 2 h followed by TNF α (100 ng/ml), or treated with shikonin (0.5 μ M), or pre-treated with RIP1 inhibitor GSK481 (300 nM) for 2 h followed by shikonin (0.5 μ M), or necrostatin-1 (60 μ M) for 2 h followed by shikonin (0.5 μ M), or zVAD (20 μ M) for 2 h followed by shikonin (0.5 μ M) to induce or block necroptosis and apoptosis respectively. Cells were labelled with fixable live cell stain Zombie NIR, Caspase-3-BV650/605 and RIP3-PE as described in Materials and Methods. After gating as described in Fig. 1 live and dead cells were further gated for necroptosis, RIP1-dependent apoptosis and apoptosis respectively using a dot-plot of RIP3-PE v Caspase-3-BV650/605 parameters. Necroptosis was described as an up-regulation of RIP3 in the RIP3-PE⁺/Caspase-3-BV650^{-ve} or BV605^{-ve} population. Median MFI values from flow cytometric and Imagestream analysis were expressed as MFI \pm SEM for n = 3. Imagestream analysis of live cells showed the RIP3-PE distribution within such cells as well as the brightfield image using x40 magnification. Student *t* tests were performed in GraphPad software with *P* = >.05 not significant (NS), *P* = <.05*, *P* = <.01**, Not Done (ND).

The degree of these phenotypes in the dead cell population induced by TNF α were shown to be for necroptotic phenotype (RIP3⁺/Caspase-3^{-ve}) were RIP3 was up-regulated by 26% (8 \pm 3.1%; TNF α RIP3 MFI 188,516 \pm 47,477; untreated 149,817 \pm 47,477), apoptosis (36.4 \pm 10.7%) and RIP1-dependent apoptosis (27 \pm 5.4%, see Fig. 2D). Imagestream analysis of dead TNF α induced necroptosis showed the up-regulation of RIP3 by 88% (untreated MFI 147,000; TNF α MFI 277,000), RIP1-dependent apoptosis, apoptosis and granular morphology changes associated with necroptosis or apoptosis respectively (Supplementary Fig. 3A, B, 4B, D, Fig. 4B, D). Interestingly a fourth form of cell death was revealed as a double negative (DN) population (non-apoptotic-necroptotic phenotype) of cells which increased after TNF α treatment with 2 8.6 \pm 6.7% compared to controls (21 \pm 5.2%, see Fig. 2B, D, Table 2). These DN cells also had low values for cell diameter, perimeter and circularity by Imagestream morphological analysis (data not shown).

We then employed the necroptotic drug shikonin which has also been previously reported to induce apoptosis [20,26]. The live cell population showed up-regulation of RIP3 to a lower level by flow (215,524 \pm 8683 MFI or by 17 \pm 4%) and image (180,000 \pm 17,600 MFI or by 20 \pm 10%) cytometry than that induced by TNF α (flow 34 \pm 10%; Image 55% \pm 15%), see Fig. 3. Similar levels of apoptosis (RIP3^{-ve}/Caspase-3⁺) were induced by shikonin as by TNF α (18.2 \pm 6.1%, Fig. 2E). A large increase in RIP1-dependent apoptosis and double negative cells was induced by shikonin compared to TNF α , 25.8 \pm 8.8 and 24.4 \pm 8.6% respectively, (Fig. 2E, Table 2). The dead cells after shikonin treatment showed high levels of RIP3 expression in the small necroptotic population (MFI 232,000 \pm 23,878, 55% up-regulation) RIP1-dependent apoptosis and apoptosis similar to TNF α treatment (Fig. 2F).

Induction of apoptosis by etoposide showed a high level of RIP3^{-ve}/Caspase-3⁺ cells (37.4 \pm 7.2%, Fig. 2G, Table 2). It was interesting to note that when the cells are expressing caspase-3 there are very few cells expressing only RIP3 (13.2 \pm 4.6), see Fig. 2G). Only when the cells undergo RIP1-dependent apoptosis

does the RIP3 expression return (26 \pm 6.8%, Fig. 2G). The dead cells induced by etoposide treatment also showed these levels of cell apoptosis (33.6 \pm 6.1%), RIP1-dependent apoptosis (30.4 \pm 6.7%) and double negative cells, 33.4 \pm 8.3% (RIP3^{-ve}/Caspase-3^{-ve}), see Fig. 2H. Image analysis of etoposide treated live and dead RIP3^{-ve}/Caspase-3⁺ cells showed the morphology of apoptotic cells (Supplementary Fig. 4K, L).

3.3. Flow cytometric and Imagestream analysis of the inhibition of RIP1 and apoptosis with TNF α and shikonin treatments

The RIP1 inhibitor GSK481 ablated the up-regulation of RIP3 in live cells by TNF α without any change in the level of RIP1-dependent apoptosis and apoptosis as determined by flow and image cytometry (Figs. 3, 5A, Table 1). Imagestream analysis also showed the down-regulation of RIP3 and cell morphology which was surprisingly like that observed with necroptosis (Fig. 3). While live RIP1-dependent apoptotic and apoptotic cells displayed caspase-3 and an apoptotic cell morphology respectively (Fig. 4E, Supplementary Fig. 4E). Again the distribution of necroptosis (RIP3 down-regulated, MFI 127,295 \pm 24,808), RIP1-dependent apoptosis and apoptosis did not change in dead cells (Figs. 2D, 5B). Imagestream analysis of dead necroptotic showed down-regulation of RIP3 (MFI 122,000), RIP1-dependent apoptotic and apoptotic cells showed RIP3, caspase-3, Zombie NIR and necroptotic or apoptotic cell morphology respectively (Supplementary Fig. 3C, 4F, Fig. 4F).

Likewise RIP1 inhibitor GSK481 stopped RIP3 up-regulation in live cells induced by shikonin (by flow and image cytometry) with no change in the incidence of RIP1-dependent apoptosis (21.3 \pm 5.2%, Figs. 3, 6A, Table 1). Unlike the RIP1 inhibitor GSK481 blockade of TNF α , shikonin produced as expected a large increase in apoptosis (RIP3^{-ve}/Caspase-3⁺, 33.7 \pm 3.1%, Fig. 6A). Dead cells not only showed a high level of apoptosis (RIP3^{-ve}/Caspase-3⁺, 43.3 \pm 5.4%) but also a large rise in the double negative cells (28.3 \pm 6.8%, Fig. 6B).

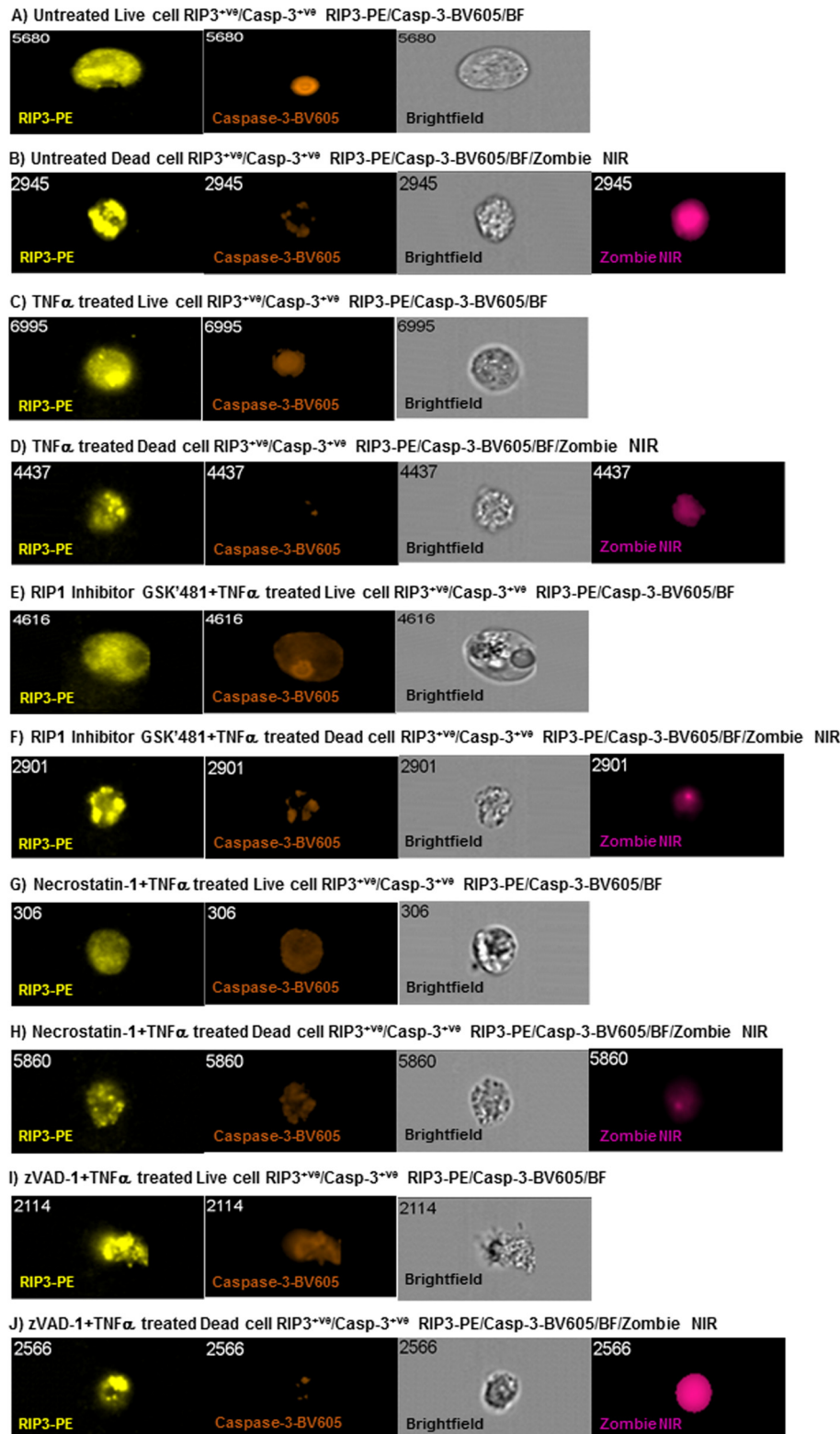


Fig. 4. Cells were untreated, live and dead (A), (B), or treated with TNF α (100 ng/ml) (C), (D), or pre-treated with RIP1 inhibitor GSK'481 (300 nM) for 2 h followed by TNF α (100 ng/ml) (E), (F), or necrostatin-1 (60 μ M) for 2 h followed by TNF α (100 ng/ml) (G), (H) or zVAD (20 μ M) for 2 h followed by TNF α (100 ng/ml) (I), (J) to induce or block necroptosis and apoptosis respectively. Cells were labelled with fixable live cell stain Zombie NIR, Caspase-3-BV605 and RIP3-PE as described in Materials and Methods. After gating as described in Supplementary Fig. 2 live and dead cells were further gated for necroptosis, RIP1-dependent apoptosis and apoptosis respectively using a dot-plot of RIP3-PE vs Caspase-3-BV605 parameters. RIP1-dependent apoptosis RIP3-PE⁺/Caspase-3-BV605⁺ population of live and dead cells were imaged by Imagestream analysis which showed the RIP3-PE/Caspase-3-BV605/Zombie NIR distribution within such cells as well as the brightfield image (BF) using $\times 40$ magnification.

In contrast to GSK'481, RIP1 inhibition of TNF α by necrostatin-1 did not alter the distribution of cell populations compared to that observed with TNF α alone, see Figs. 2C, D, 5C, D, Table 1. As

expected necroptosis was inhibited as indicated by the down-regulation of RIP3 ($P < .01$) in live and dead RIP3⁺ events (Figs. 3, 5C, D). Imagestream analysis of live and dead RIP3⁺ cells also

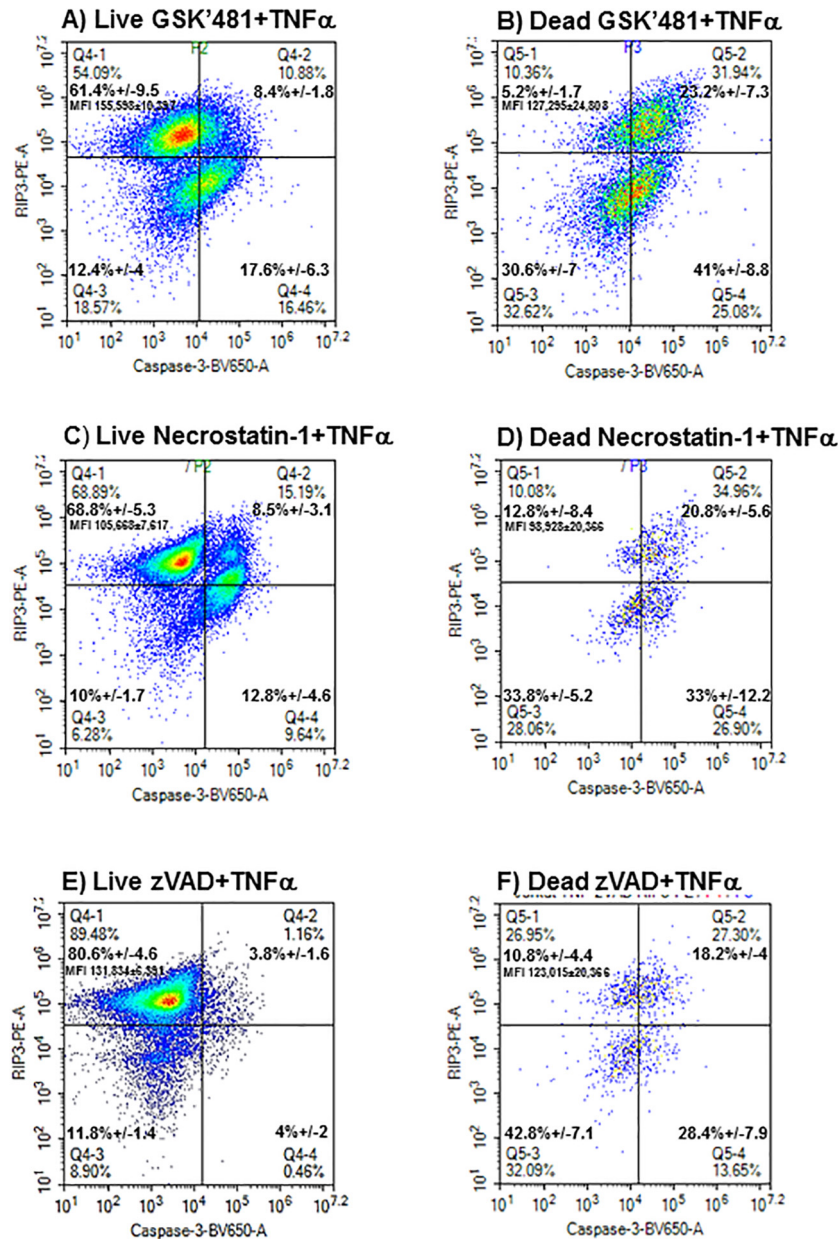


Fig. 5. Cells were pre-treated with RIP1inhibitor GSK'481 (300 nM) for 2 h followed by TNF α (100 ng/ml) (A) live cells, (B) dead cells, or necrostatin-1 (60 μ M) for 2 h followed by TNF α (100 ng/ml) (C), (D) or zVAD (20 μ M) for 2 h followed by TNF α (100 ng/ml) (E), (F) to block necroptosis and apoptosis respectively. Cells were labelled with fixable live cell stain Zombie NIR, Caspase-3-BV650 and RIP3-PE as described in Materials and Methods. After gating as described in Fig. 1 live and dead cells were further gated for necroptosis, RIP1-dependent apoptosis and apoptosis respectively using a dot-plot of RIP3-PE vs Caspase-3-BV650 parameters. Necroptosis was described as an up-regulation of RIP3 in the RIP3-PE^{ve}/Caspase-3-BV650^{ve} population. RIP1-dependent apoptosis and was described as the RIP3-PE^{ve}/Caspase-3-BV650^{ve} or RIP3-PE^{ve}/Caspase-3-BV650^{ve} population. Mean percentage values were expressed as % \pm SEM, MFI were median values \pm SEM for RIP3^{ve}/Caspase-3^{ve}, SEM for n = 3.

showed the down-regulation of RIP3 and necroptotic like cell morphology (Fig. 3, Supplementary Fig. 3D). Image analysis of live and dead apoptotic and RIP1-dependent apoptotic cells showed the presence of RIP3, Caspase-3 \pm Zombie NIR and apoptotic cell morphology (Supplementary Fig. 4G, H, Fig. 4G, H).

Necrostatin-1 also inhibited necroptosis induced by shikonin as indicated by the down-regulation of RIP3 expression (Figs. 3, 6C, $P < .01$, Table 1). Necrostatin-1 also induced changes in the distribution of cell death modes with an increase in apoptosis (Caspase-3^{ve}/RIP3^{ve} 29.8% \pm 4.1) in live cells (Fig. 6C) with no change in the distribution of dead cells (Fig. 6D).

Live cells showed abrogation of RIP3 up-regulation by TNF α in the presence of zVAD by flow and image cytometry but all the cells

remained mainly RIP3^{ve} and had a necroptotic like cell morphology see Figs. 3, 5E, $P < .01$, Table 1. Imagestream analysis of remaining apoptotic and RIP1-dependent apoptotic cell populations not only showed the presence of RIP3, and caspase-3 but apoptotic cell morphology (Fig. 4I, Supplementary Fig. 4I).

Similarly dead cells generated from TNF α -zVAD treatment showed a high degree of necroptosis (10.8 \pm 4.4%, RIP3^{ve}/Caspase-3^{ve}), but surprisingly RIP1-dependent apoptosis (double positive, 18.2 \pm 4%) and even apoptosis (28.4 \pm 7.9%, Caspase-3^{ve}), as well as double negative cells (42.8 \pm 7.1%, see Fig. 5F). Image analysis of dead necroptotic cells showed the presence of RIP3, Zombie NIR and a necroptotic like cell morphology (Supplementary Fig. 3E). While dead apoptotic and RIP1-dependent

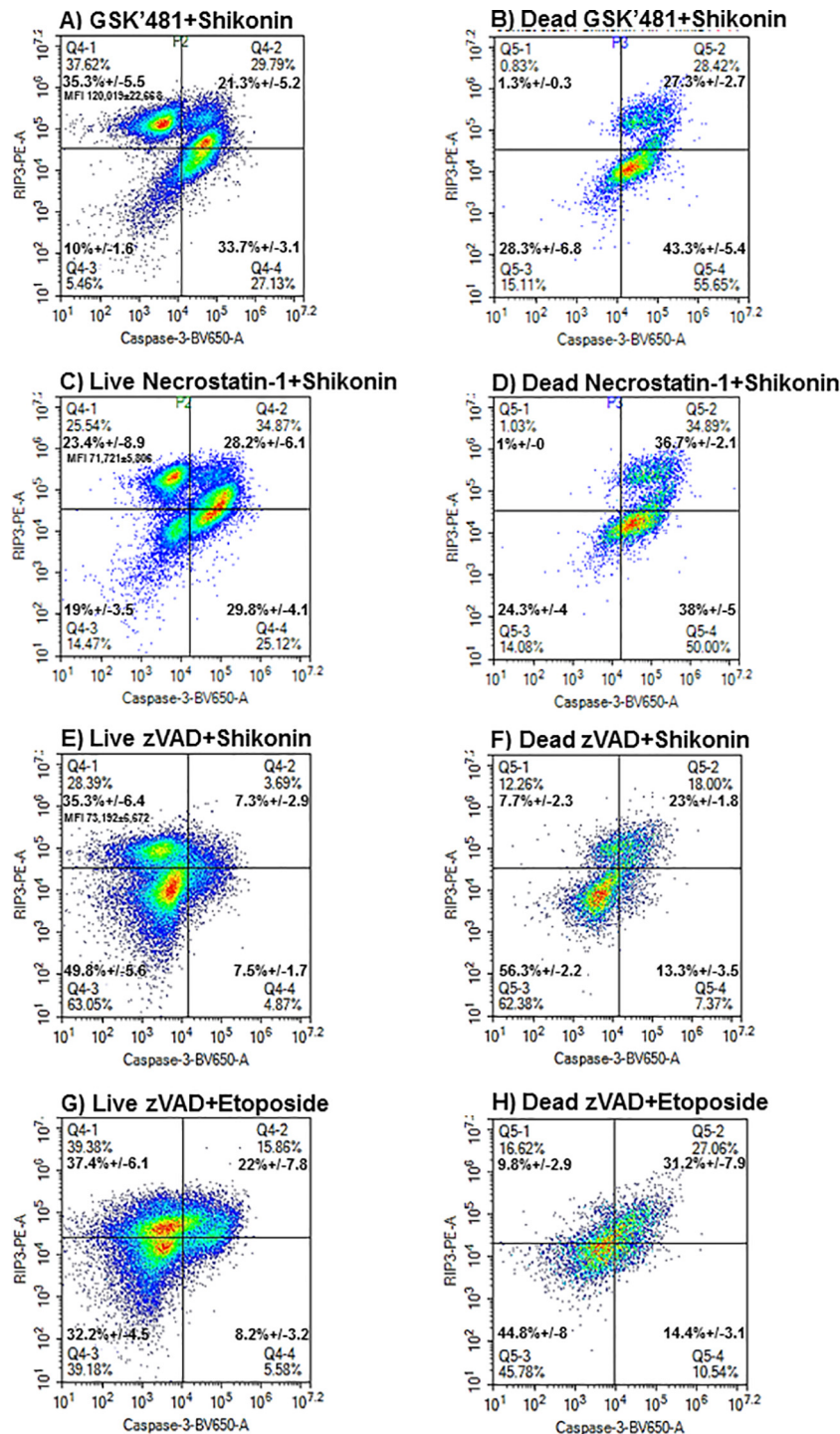


Fig. 6. Cells were pre-treated with RIP1 inhibitor GSK'481 (300 nM) for 2 h followed by shikonin (0.5 μ M) (A) live cells, (B) dead cells, or necrostatin-1 for 2 h followed by shikonin (0.5 μ M) (C), (D) or zVAD (20 μ M) for 2 h followed by shikonin (0.5 μ M) (E), (F) to block necroptosis and apoptosis respectively. Cells were labelled with fixable live cell stain Zombie NIR, Caspase-3-BV650 and RIP3-PE as described in Materials and Methods. After gating as described in Fig. 1 live and dead cells were further gated for necroptosis, RIP1 dependent apoptosis and apoptosis respectively using a dot-plot of RIP3-PE v Caspase-3-BV650 parameters. Necroptosis was described as an up-regulation of RIP3 in the RIP3-PE^{ve}/Caspase-3-BV650^{ve} population. RIP1-dependent apoptosis was described as the RIP3-PE^{ve}/Caspase-3-BV650^{ve} population. Apoptosis was described as the RIP3-PE^{ve}/Caspase-3-BV650^{ve} population. Mean percentage values were expressed as % \pm SEM, MFI were median values \pm SEM for RIP3-PE, SEM for n = 3.

apoptotic cells showed the presence of caspase-3 and an apoptotic or much shrunken cell morphology respectively (Supplementary Fig. 4J, Fig. 4J).

The zVAD pre-treatment with shikonin also inhibited RIP3 upregulation in live cells. However, not all cells were RIP3^{ve}/Caspase-3^{ve} as there was a high incidence of the double negative phenotype (49.8% \pm 5.6) (Figs. 3, 6E, $P < .01$, Table 1). Treatment with

zVAD-shikonin resulted in little apoptosis in the dead cell population but led to a degree of RIP1-dependent apoptosis (23 \pm 1.8%) and again a high incidence of double negative cells (56.3 \pm 2.2%), see Fig. 6F.

Interestingly zVAD blockade of etoposide maintained the RIP1-dependent apoptotic phenotype (22 \pm 7.8%) displayed with etoposide alone, and also induced a live double negative population of

cells ($32.2 \pm 4.5\%$, Fig. 6G, Table 1). This double negative population was enhanced and RIP1-dependent apoptosis was maintained in such treated dead cells respectively ($44.8 \pm 8\%$, $31.2 \pm 7.9\%$, Fig. 6H).

4. Discussion

The use of DNA dyes to detect apoptosis and cell death in the 80's by the use of cell permeant Hoechst 33342 together with PI required the need for an expensive UV laser line. This was then replaced by the now ubiquitous annexin V flow cytometric assay and has been in use since the mid-90's [19]. This assay has been extremely useful in the study of apoptosis particularly when combined with cell permeant probes for mitochondrial function, caspase active probes such as FLICA (Fluorescent Inhibitor Caspases) and ROS detection probes. However, its application to the study of other forms of cell death such as necroptosis and RIP1-dependent apoptosis has shown the limitations of the annexin V binding assay given it's non-specific nature [13,16,27,28].

The mainstay techniques for investigating cell death pathways has been Western Blot and fluorescence microscopy technology which has elucidated the proteins involved in apoptosis and other forms of cell death such as necroptosis and RIP1 dependent apoptosis amongst the other now recognized forms of cell death [20–22]. Reviews of the technologies available for the study of cell death mechanisms have shown there is no one perfect approach [13]. Western blotting shows only the predominant proteins involved in any one form of cell death, with the nuances of other active signalling routes not shown due to the low incidence of any one particular form of cell death. While microscopy although it can distinguish live and dead cells and presence of apoptotic and necroptotic cells in such populations it lacks the in-depth analysis of all populations that image and flow cytometry offers.

This new flow cytometric assay employing the simple use of directly conjugated mAbs (that bind to antigen in fixed as opposed to lysed cell samples) reveals the known complexity of cell death processes induced by particular cell death inducing agents (e.g. TNF α , shikonin and etoposide). The backbone of the new assay not only showed cell populations undergoing apoptosis by being only caspase-3⁺ but showed that non-viable cells have either reached this point via apoptosis (Caspase-3⁺/Zombie dye⁺) or by a mechanism via RIP3. The addition of a second antibody against RIP3, a protein that is up-regulated in necroptosis added the extra dimension to the assay to definitively demonstrate cell death phenotypes of the cells involved in necroptosis, apoptosis and RIP1-dependent apoptosis while the cells were still viable, but also for the first time in the dead cell population. TNF α and shikonin treatments of Jurkat cells showed the presence of apoptosis (Caspase-3⁺/RIP3⁻), but also necroptosis by the up-regulation of RIP3 in the RIP3⁺/Caspase-3⁻ populations of live and dead cells [10]. As expected, etoposide induced an increase in live cells with a RIP3⁻/Caspase-3⁺ phenotype indicating apoptosis, but also showed the presence of a RIP1-dependent apoptotic phenotype (Caspase-3⁺/RIP3⁺) [10]. However all dead cells including controls showed the same relative distribution of all forms of cell death studied. This immunophenotypic analysis of RIP3-PE, Caspase-3-BV650/605 and Zombie NIR to identify necroptosis, RIP1-dependent apoptosis and apoptosis was further confirmed by Imagestream analysis and by the use of specific inhibitors to block necroptosis and apoptosis. Image analysis of the distribution of RIP3 in the necroptotic populations showed no defining patterns or characteristics other than a general increase in MFI. These Imagestream RIP3 MFIs compared well with the corresponding flow cytometry MFIs (see Fig. 3.) Morphological analysis of cells (untreated or with any treatment) by image cytometry showed

only a similar shrinkage in cells in the RIP3 negative populations of cells which included apoptotic and double negative cells by diameter, perimeter and circularity and thus unfortunately was of no specific use.

The inhibition of necroptotic and apoptotic cell death signalling routes by employing a RIP1 inhibitors, GSK481 [25] and necrostatin-1 [29–31] as well as pan caspase blocker zVAD, gave illuminating insight to the changes in the RIP3/Caspase-3 populations. Cell cultures treated with TNF α and shikonin were shown to promote apoptosis and necroptosis [32–34]. GSK481 abrogated the RIP3 up-regulation induced by both TNF α and shikonin in live and dead cells, indicating that necroptosis was in fact induced by both agents. The overall levels of cell death were unchanged, however increased Caspase-3⁺ levels were observed in conjunction with shikonin but not TNF α [25,29]. Necroptosis induced by TNF α and shikonin was also shown to be blocked by necrostatin-1 [30,31]. These differences observed with the different RIP1 inhibitors appeared to possibly reflect the differences in the signalling routes activated by TNF α and shikonin. In contrast dead cells from both such treatments indicated cell death from apoptosis and RIP1-dependent apoptosis and surprisingly the double negative cell death (RIP3⁻/Caspase-3⁻) in the case of shikonin treated cells.

Further elucidation of the interconnections between cell death pathways was investigated by the use of pan caspase blocker zVAD together with TNF α or shikonin which has been reported to increase necroptosis [31,33,34]. There was reduced caspase-3 levels in tandem with the viability levels of the cells compared to single drug treatments. The outcome of such treatments was surprisingly different with TNF α -zVAD live cells displaying a small degree of down regulation of resting levels of RIP3. However zVAD treatment with shikonin showed a massive down regulation of RIP3 with the preponderance of a double negative phenotype. Why should a down regulation of RIP3 be observed in such live cells treated to undergo necroptosis when all other responses to the modulation of RIP3 and population dynamics meet the expected changes? The treatment with Etoposide \pm zVAD however provides an insight into this issue as it was initially shown to down-regulate the RIP3 machinery, while the remaining RIP3⁺/Caspase-3⁻ population showed a down-regulation of RIP3. This new assay therefore does appear to shed new light on the observed expressions of proteins involved in cell death processes which are not highlighted by Western Blot data. The dead cell phenotype of such treated cells showed the maintenance of a double negative population, thus these cells appear to have undergone a non-apoptotic-necroptotic form of cell death. Interestingly cell death after etoposide-zVAD treatment also showed cells undergoing cell death with this double negative phenotype and RIP1-dependent apoptosis.

This new flow cytometric approach uses antibodies to phenotypically analyse cell death into eight parts thus revealing up till now undetectable minor (but significant) as well as major cell populations undergoing varying degrees of necroptosis, apoptosis and RIP1-dependent apoptosis when the cells are alive and dead. Interestingly shikonin was shown to induce a higher degree of apoptosis than TNF α as well as necroptosis. The use of RIP1 and pan-caspase inhibitors clearly revealed the signalling routes activated by TNF α /shikonin and etoposide with image analysis of such cells being used to clarify the mode of cell death occurring. Given that the assay requires only 125,000 cells per test it has been possible to detect and investigate the cell death phenotypes in leucocytes isolated from resected human colon tissue (unpublished observations). The addition of other known markers for other forms of cell death are currently in the process of being added to the current assay, these include pyroptosis, autophagy, parthanatos, DNA damage and ER stress. This may lead flow cytometry technology to the fore once more in research into cell death signalling mechanisms.

Funding

This research did not receive any specific grant from funding agencies in the public, commercial, or not-for-profit sectors.

Thank you to Dr. Philip Harris and Dr. Mike Reilly (GSK, Colleagueville, PA) for their kind permission to use and publish data relating to RIP1 inhibitor GSK481. The Imagestream Mk II instrument was purchased by funding from the Wellcome Trust grant 101604/Z/13/Z.

Appendix A. Supplementary data

Supplementary data associated with this article can be found, in the online version, at <https://doi.org/10.1016/j.ymeth.2017.10.013>.

References

- [1] J.F. Kerr, A.H. Wyllie, A.R. Currie, Apoptosis: a basic biological phenomenon with wide-ranging implications in tissue kinetics, *Br. J. Cancer* 26 (1972) 239–257.
- [2] Z. Darzynkiewicz, G. Juan, X. Li, W. Gorczyca, T. Murakami, F. Traganos, Cytometry in cell necrobiology: analysis of apoptosis and accidental cell death (necrosis), *Cytometry A* 27 (1997) 1–20.
- [3] D. Wlodkowic, J. Skommer, Z. Darzynkiewicz, Cytometry in cell necrobiology revisited. Recent advances and new vistas, *Cytometry A* 77A (2010) 591–606.
- [4] S.L. Fink, B.T. Cookson, Apoptosis, pyroptosis, and necrosis: mechanistic description of dead and dying eukaryotic cells, *Infect. Immun.* 73 (2005) 1907–1916.
- [5] L. Galluzzi, J.M. Bravo-San Pedro, I. Vitale, S.A. Aaronson, J.M. Abrams, D. Adam, E.S. Alnemri, L. Altucci, D. Andrews, M. Annicchiarico-Petruzzelli, E.H. Baehrecke, N.G. Bazan, M.J. Bertrand, K. Bianchi, M.V. Blagosklonny, K. Blomgren, C. Borner, D.E. Bredesen, C. Brenner, M. Campanella, E. Candi, F. Cecconi, F.K. Chan, N.S. Chandel, E.H. Cheng, J.E. Chipuk, J.A. Cidlowski, A. Ciechanover, T.M. Dawson, V.L. Dawson, V. De Laurenzi, R. De Maria, K.M. Debatin, N. Di Daniele, V.M. Dixit, B.D. Dynlacht, W.S. El-Deiry, G.M. Fimia, R.A. Flavell, S. Fulda, C. Garrido, M.L. Gougeon, D.R. Green, H. Gronemeyer, G. Hajnóczky, J.M. Hardwick, M.O. Hengartner, H. Ichijo, B. Joseph, P.J. Jost, T. Kaufmann, O. Kepp, D.J. Klionsky, R.A. Knight, S. Kumar, J.J. Lemasters, B. Levine, A. Linkermann, S.A. Lipton, R.A. Lockshin, C. Lopez-Otin, E. Lugli, F. Madeo, W. Malorni, J.C. Marine, S.J. Martin, J.C. Martinou, J.P. Medema, P. Meier, S. Melino, N. Mizushima, U. Moll, C. Munoz-Pinedo, G. Nunez, A. Oberst, T. Panaretakis, J.M. Penninger, M.E. Peter, M. Piacentini, P. Pintun, J.H. Prehn, H. Puthalakath, G.A. Rabinovich, K.S. Ravichandran, R. Rizzuto, C.M. Rodrigues, D.C. Rubinsztein, T. Rudel, Y. Shi, H.U. Simon, B.R. Stockwell, G. Szabadkai, S.W. Tait, H.L. Tang, N. Tavernarakis, Y. Tsumimoto, T. Vanden Berghe, P. Vandenabeele, A. Villunger, E.F. Wagner, H. Walczak, E. White, W.G. Wood, J. Yuan, Z. Zakeri, B. Zhivotovsky, G. Melino, G. Kroemer, Essential versus accessory aspects of cell death: recommendations of the NCCD 2015, *Cell Death Differ.* 22 (2015) 58–73.
- [6] D.R. Green, F. Llambi, Cell Death Signaling, *Cold Spring Harb. Perspect. Biol.* 7 (2015).
- [7] L. Galluzzi, I. Vitale, J.M. Abrams, E.S. Alnemri, E.H. Baehrecke, M.V. Blagosklonny, T.M. Dawson, V.L. Dawson, W.S. El-Deiry, S. Fulda, E. Gottlieb, D.R. Green, M.O. Hengartner, O. Kepp, R.A. Knight, S. Kumar, S.A. Lipton, X. Lu, F. Madeo, W. Malorni, P. Mehlen, G. Nun, M.E. Peter, M. Piacentini, D.C. Rubinsztein, Y. Shi, H.U. Simon, P. Vandenabeele, E. White, J. Yuan, B. Zhivotovsky, G. Melino, G. Kroemer, Molecular definitions of cell death subroutines: recommendations of the Nomenclature Committee on Cell Death 2012, *Cell Death Differ.* 19 (2012) 107–120.
- [8] J.C. Martinou, R.J. Youle, Mitochondria in apoptosis: Bcl-2 family members and mitochondrial dynamics, *Dev. Cell* 21 (2011) 92–101.
- [9] S. Yonehara, A. Ishii, M. Yonehara, A cell-killing monoclonal antibody (anti-Fas) to a cell surface antigen co-down regulated with the receptor of tumor necrosis factor, *J. Exp. Med.* 169 (1989) 1747–1756.
- [10] M. Conrad, J.P. Angeli, P. Vandenabeele, B.R. Stockwell, Regulated necrosis: disease relevance and therapeutic opportunities, *Nat. Rev. Drug Discov.* 15 (2016) 348–366.
- [11] D. Ofengeim, J. Yuan, Regulation of RIP1 kinase signalling at the crossroads of inflammation and cell death, *Mol. Cell Biol.* 14 (2013) 727–736.
- [12] S.W. Tait, G. Ichim, D.R. Green, Die another way-non-apoptotic mechanisms of cell death, *J. Cell Sci.* 127 (2014) 2135–2144.
- [13] L. Galluzzi, S.A. Aaronson, J. Abrams, E.S. Alnemri, D.W. Andrews, E.H. Baehrecke, N.G. Bazan, M.V. Blagosklonny, K. Blomgren, C. Borner, D.E. Bredesen, C. Brenner, M. Castedo, J.A. Cidlowski, A. Ciechanover, G.M. Cohen, V. De Laurenzi, R. De Maria, M. Deshmukh, B.D. Dynlacht, W.S. El-Deiry, R.A. Flavell, S. Fulda, C. Garrido, P. Golstein, M.L. Gougeon, D.R. Green, H. Gronemeyer, G. Hajnóczky, J.M. Hardwick, M.O. Hengartner, H. Ichijo, M. Jaattela, O. Kepp, A. Kimchi, D.J. Klionsky, R.A. Knight, S. Kornbluth, S. Kumar, B. Levine, S.A. Lipton, E. Lugli, F. Madeo, W. Malorni, J.C. Marine, S.J. Martin, J.P. Medema, P. Mehlen, G. Melino, U.M. Moll, E. Morselli, S. Nagata, D.W. Nicholson, P. Nicotera, G. Nunez, M. Oren, J. Penninger, S. Pervaiz, M.E. Peter, M. Piacentini, J.H. Prehn, H. Puthalakath, G.A. Rabinovich, R. Rizzuto, C.M. Rodrigues, D.C. Rubinsztein, T. Rudel, L. Scorrano, H.U. Simon, H. Steller, J. Tschopp, Y. Tsumimoto, P. Vandenabeele, I. Vitale, K.H. Vousden, R.J. Youle, J. Yuan, B. Zhivotovsky, G. Kroemer, Guidelines for the use and interpretation of assays for monitoring cell death in higher eukaryotes, *Cell Death Differ.* 16 (2009) 1093–1107.
- [14] J. Sosna, S. Voigt, S. Mathieu, A. Lange, L. Thon, P. Davarnia, T. Herdegen, A. Linkermann, A. Rittger, F.K.M. Chan, D. Kabelitz, S. Schütze, D. Adam, TNF induced necroptosis and PARP 1 mediated necrosis represent distinct routes to programmed necrotic cell death, *Cell. Mol. Life Sci.* 71 (2014) 331–348.
- [15] C.M. Henry, E. Hollville, S.J. Martin, Measuring apoptosis by microscopy and flow cytometry, *Methods Cell Biol.* 61 (2013) 90–97.
- [16] M.E. Christensen, E.S. Jansen, W. Sanchez, N.J. Waterhouse, Flow cytometry based assays for the measurement of apoptosis-associated mitochondrial membrane depolarisation and cytochrome c release, *Methods* 61 (2013) 138–145.
- [17] D. Wlodkowic, W. Telford, J. Skommer, Z. Darzynkiewicz, Apoptosis and beyond: cytometry in studies of programmed cell death, *Methods Cell Biol.* 103 (2011) 55–98.
- [18] O. Kepp, L. Galluzzi, M. Lipinski, J. Yuan, G. Kroemer, Cell death assays for drug discovery, *Nat. Rev. Drug Discov.* 10 (2011) 221–237.
- [19] I. Vermes, C. Haanen, H. Steffens-Nakken, C. Reutelingsperger, A novel assay for apoptosis flow cytometric detection of phosphatidylserine early apoptotic cells using fluorescein labelled expression on Annexin V, *J. Immunol. Methods* 184 (1995) 39–51.
- [20] Z. Fu, B. Deng, Y. Liao, L. Shan, F. Yin, Z. Wang, H. Zeng, D. Zuo, Y. Hua, Z. Cai, The anti-tumor effect of shikonin on osteosarcoma by inducing RIP1 and RIP3 dependent necroptosis, *BMC Cancer* 13 (2013) 580–590.
- [21] J. Karch, O. Kanisičak, M.J. Brody, M.A. Sargent, D.M. Michael, J.D. Molkenin, Necroptosis interfaces with MOMP and the MPTP in mediating cell death, *PLoS One* (2015) 1–12.
- [22] S. McComb, H.H. Cheung, R.G. Korneluk, S. Wang, L. Krishnan, S. Sad, cIAP1 and cIAP2 limit macrophage necroptosis by inhibiting Rip1 and Rip3 activation, *Cell Death Differ.* 19 (2012) 1791–1801.
- [23] W. Han, L. Li, S. Qiu, Q. Lu, Q. Pan, Y. Gu, J. Luo, X. Hu, Shikonin circumvents cancer drug resistance by induction of a necroptotic death, *Mol. Cancer Ther.* 6 (2007) 1641–1649.
- [24] I.A. Vorobjev, N.S. Barteneva, Multi-parametric imaging of cell heterogeneity in apoptosis analysis, *Methods* 112 (2017) 105–123.
- [25] P.A. Harris, B.W. King, D. Bandyopadhyay, S.B. Berger, N. Campobasso, C.A. Capriotti, J.A. Cox, L. Dare, X. Dong, J.N. Finger, L.C. Grady, S.J. Hoffman, J.U. Jeong, J. Kang, V. Kasparcova, A.S. Lakdawala, R. Lehr, D.E. McNulty, R. Nagilla, M.T. Ouellette, C.S. Pao, A.R. Rendina, M.C. Schaeffer, J.D. Summerfield, B.A. Swift, R.D. Totoritis, P. Ward, A. Zhang, D. Zhang, R.W. Marquis, J. Bertin, P.J. Gough, DNA-encoded library screening identifies benzo[b][1,4]oxazepin-4-ones as highly potent and monoselective receptor interacting protein 1 kinase inhibitors, *J. Med. Chem.* 59 (2016) 2163–2178.
- [26] B. Wiench, T. Eichhorn, M. Paulsen, T. Efferth, Shikonin directly targets mitochondria and causes mitochondrial dysfunction in cancer cells, *Evid. Based Complement Alternat. Med.* 2012 (2012) 726025.
- [27] A. Rasola, M. Genuna, A flow cytometry assay simultaneously detects independent apoptotic parameters, *Cytometry A* 45 (2001) 151–157.
- [28] E. Lugli, L. Troaino, R. Ferraresi, E. Roat, N. Prada, M. Nasi, M. Pinti, E.L. Cooper, A. Cossaizza, Characterization of c cells with different mitochondrial membrane potential during apoptosis, *Cytometry A* 68A (2005) 28–35.
- [29] T. Xie, W. Peng, Y. Liu, C. Yan, J. Maki, A. Degtarev, J. Yuan, Y. Shi, Structural basis of RIP1 inhibition by necrostatins, *Structure* 21 (2013) 493–499.
- [30] W. Han, J. Xie, Y. Fang, Z. Wang, H. Pan, Nec-1 enhances shikonin-induced apoptosis in leukemia cells by inhibition of RIP-1 and ERK1/2, *Int. J. Mol. Sci.* 13 (2012) 7212–7225.
- [31] T. McQuade, Y. Cho, F.K.M. Chan, Positive and negative phosphorylation regulates RIP1 and RIP3-induced programmed necrosis, *Biochem. J.* 456 (2013) 409–415.
- [32] H. Sawai, Induction of apoptosis in TNF-treated L929 cells in the presence of necrostatin-1, *Int. J. Mol. Sci.* 17 (2016).
- [33] L. Galluzzi, O. Kepp, S. Krautwald, G. Kroemer, A. Linkermann, Molecular mechanisms of regulated necrosis, *Semin. Cell Dev. Biol.* 35 (2014) 24–32.
- [34] N. Khan, K.E. Lawlor, J.M. Murphy, J.E. Vince, More to life than death: molecular determinants of necroptotic and non-necroptotic RIP3 kinase signaling, *Curr. Opin. Immunol.* 26 (2014) 76–89.